UFMC-based Wideband Spectrum Sensing for Cognitive Radio Systems in Non-Gaussian Noise

Djamel E. Kebiche[1], Ali Baghaki[1], Xiaomei Zhu[2], and Benoit Champagne[1]
[1]Dept. of Electrical and Computer Eng., McGill University, Montreal, Canada
[2] Inst. of Signal Proc. and Transmission, Nanjing Univ. of Posts and Telecomm., Nanjing, China
Email: {djamel.kebiche, ali.baghaki}@mail.mcgill.ca; njiczxm@njut.edu.cn; benoit.champagne@mcgill.ca

***Abstract*—Cognitive radio (CR) is an important technology that allows to deal with spectrum congestion, where secondary applications (users) attempt to access a frequency band that is reserved for a primary application. A challenging function for a CR is to sense a frequency band and detect the absence or presence of a licensed user, a task referred to as *spectrum sensing*. In this paper, we investigate the performance of the Rao-test based detector for wideband spectrum sensing under non-Gaussian noise in a multi-carrier transmission framework. Specifically, we incorporate this detector into the universal filtered multicarrier (UFMC) modulation scheme envisaged for 5G systems. Through numerical simulations, we show that the Rao-test based detector combined with UFMC outperforms the traditional OFDM based system in a realistic non-Gaussian noise environment.**

I. Introduction

Cognitive radio (CR) has emerged as an innovative solution to the spectrum congestion problem by enabling opportunistic usage of frequency bands that are not heavily used by licensed users [1]-[2]. In the context of CR, *primary users* (PU) are defined as licensed users who have a higher priority on the usage of a specific part of the spectrum. *Secondary users* (SU) are unlicensed CR users who can exploit the spectrum in a non-interfering manner to PUs. Within this context, spectrum sensing refers to the task of detecting PUs and determining spectrum availability for SUs in the CR network.

Several modern spectrum sensing techniques have been developed that exploit various properties of the PU and noise signals to allow one or more SUs to detect the presence of PUs. The authors in [3] present a *matched filter* detection approach while a cyclostationary detection method that exploits periodicity features of PU signals is presented in [4]. Although these and other related methods can achieve good detection performance under low signal-to-noise ratio (SNR), they make strong assumptions about available *a priori* knowledge of the PU signal shape or features. Spectrum sensing based on energy detection is the most recurrent technique in practice because of its low computational complexity and minimal use of *a priori* information [5]. However, a detector based on energy detection is optimized with respect to a Gaussian noise environment. Consequently, when non-Gaussian noise impairments are present, the detector's performance is reduced considerably. These impairments may include man-made impulse noise, co-channel interference from other SUs, out of band spectral leakage, etc. Recently, a Rao-test based detector optimized for non-Gaussian noise environments was introduced in [6] which yields an improved performance.

Wideband spectrum sensing aims to sense a frequency band that exceeds the coherence bandwidth of the wireless channel [7]. A simple approach is to divide the wideband spectrum into a series of contiguous narrower subbands, through the application of Fourier transform or filter bank techniques on the received signal. Subsequently, narrowband sensing is applied in each subband to identify individual spectral opportunities. A more sophisticated approach consists in combining test statistics from multiple subbands and performing an (optimal) joint detection of the PU signals over the larger frequency spectrum, as presented in [8]-[9]. Within this context, the use of a proper filtering scheme for separating the PU and SU signals in the frequency domain is of paramount importance.

Multicarrier modulation (MCM) techniques remain the favored option for wideband signal transmission in the physical layer of existing and future wireless systems, such as 4G and upcoming 5G networks. Among the MCM techniques, OFDM has been largely adopted in many pre-4G and 4G systems due to its simplicity of implementation. Nevertheless, OFDM suffers from

This research was jointly funded by InterDigital Canada and the Natural Sciences and Engineering Research Council (NSERC) of Canada.

The work of X. Zhu was supported by the National Natural Science Foundation of China under Grant 61372122.

978-1-5386-3531-5/17/$31.00 © 2017 IEEE

several limitations and the study of improved MCM schemes for 5G has thus attracted great interest [10]. Several filterbank multicarrier (FBMC) methods, such as filtered multitone (FMT) [11], cosine modulated multitone scheme (CMT) [12], and OFDM with offset QAM (OFDM-OQAM) [13], in which well-designed filters are used to extract the subcarrier information, have been proposed to address the shortcomings of OFDM. However, these techniques can be very complex and the required filter lengths can be very large. An alternative and promising scheme called universal filtered multicarrier (UFMC) combines the simplicity of OFDM and the advantages of FBMC [14]-[15]. Specifically, and unlike OFDM, UFMC includes a filtering operation to minimize intercarrier interference (ICI).

In this paper, we investigate the advantages of the Rao test based detector over the traditional energy detector for wideband spectrum sensing subject to non-Gaussian noise impairments in a multicarrier framework. Specifically, we extend the Rao test based detector to the wideband framework by incorporating it into the UFMC modulation scheme. We subsequently demonstrate through numerical simulations that the Rao-test based detector combined with UFMC outperforms the traditional OFDM-based detectors in a realistic non-Gaussian noise environment. Overall, the Rao detector incorporated in UFMC offers a suitable solution for wideband spectrum sensing in CR applications for future 5G networks.

The rest of this paper is organized as follows. In section II, we present the system model and review the optimal Rao-test based detector for non-Gaussian noise. In Section III, the integration of this detector within the UFMC filtering framework is decribed in details. In section IV, the detection performance of the resulting scheme for wideband spectrum sensing in non-Gaussian noise is evaluated via simulations and compared to other benchmark approaches. Finally, conclusions are drawn in Section V.

II. Optimal Detectors

In this section, we briefly review spectrum sensing detectors optimal for Gaussian and non-Gaussian additive noise environments. We consider a generic multicarrier framework where the wideband spectrum is divided into B non-overlapping narrow subbands. Some of these subbands might not be used by PUs and are therefore available for opportunistic SU access. Fig. 1 illustrates the spectrum availability for a wideband communication channel, where at a given time, some of the subbands (depicted as white rectangles) can be used opportunistically by SUs.

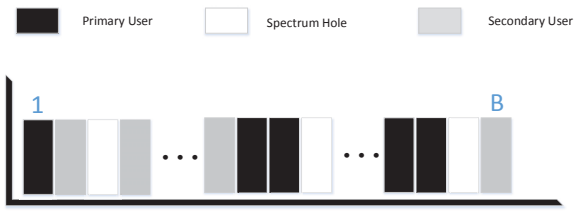

Fig. 1: Illustration of opportunistic spectrum access

A. Gaussian Noise Environment

We first consider the spectrum sensing model within a Gaussian noise environment. The decision of a particular SU on the presence or absence of a PU in subband $j \in \{1, ..., B\}$ can be formulated as a binary hypothesis testing problem as follows [8]:

$$H_{0,j} : R_j(n) = W_j(n) \quad (1)$$

$$H_{1,j} : R_j(n) = S_j(n) + W_j(n) \quad (2)$$

where $n = 0, ..., N-1$ is the discrete-time index, N is the total number of symbols in the observation window, $R_j(n)$ is the received signal sample at time n, $S_j(n)$ is the PU signal component, $W_j(n)$ is the complex additive white Gaussian noise (AWGN) with zero mean and variance σ_w^2. The SU has to decide between two hypotheses, that is: $H_{0,j}$ representing the presence of only noise in the j^{th} subband, implying that it is vacant and thus available for opportunistic access; and $H_{1,j}$ representing the presence of a PU signal with noise, implying that the j^{th} subband is occupied.

The decision on the occupancy of the j^{th} subband based on energy detection is accomplished by comparing the test statistic, denoted as T_E, against a fixed threshold λ_j which depends on the noise level. The test statistic can be expressed as follows [8]:

$$T_E\{R_j(n)\} = \sum_{n=0}^{N-1} |R_j(n)|^2 \quad (3)$$

while the decision rule is formulated as:

$$T_E\{R_j(n)\} \underset{H_{0,j}}{\overset{H_{1,j}}{\gtrless}} \lambda_j \quad (4)$$

The above test statistic, which amounts to computing the energy of the observed signal $R_j(n)$, is optimum when AWGN is present and the signal has an unknown form. However, if non-Gaussian noise impairments are present, the detector's performance is significantly reduced. Therefore, we must consider a new test statistic that can account for the non-Gaussianity of the noise.

B. General Gaussian Distributed (GGD) Noise Environment

The performance of an energy based detector optimized for additive Gaussian noise may demean considerably in the presence of non-Gaussian noise impairments due to the heavier tail characteristics of their probability density function (PDF) [17]. Indeed, the simple Gaussian noise model is not appropriate in such cases because the tail of the PDF of non-Gaussian impairments generally tend to decay at a lower rate.

Here, we assume that non-Gaussian noise can be modeled as a complex *generalized Gaussian distribution (GGD)*, thereby allowing to control the tail characteristics by means of an adjustable parameter. Specifically, the PDF of a GGD with mean μ and variance σ_w^2 is expressed as follows:

$$f_{\text{GGD}}(w;\beta) = \frac{\beta}{2A(\beta,\sigma_w^2)\Gamma(1/\beta)} e^{-\left(\frac{|w-\mu|}{A(\beta,\sigma_w^2)}\right)^{\beta}} \quad (5)$$

where

$$A(\beta,\sigma_w^2) = \left(\sigma_w^2 \frac{\Gamma(1/\beta)}{\Gamma(3/\beta)}\right)^{1/2} \quad (6)$$

$\Gamma(\nu)$ is the standard gamma function, i.e.,

$$\Gamma(\nu) = \int_0^{\infty} x^{\nu-1} \mathrm{e}^{-x} dx \quad (7)$$

and $\beta > 0$ is a shaping factor that controls the exponential decay rate of the PDF tail, allowing to model different noise behaviors. The PDF of the GGD is plotted in Fig. 2, showing the tail characteristics for different β values. The GGD reduces to the Gaussian distribution when $\beta = 2$ and to the Laplacian distribution when $\beta = 1$. Several types of noise sources found in practice tend to produce samples with higher magnitudes than what the Gaussian noise model would predict, i.e. corresponding to the case $\beta < 2$ in (5).

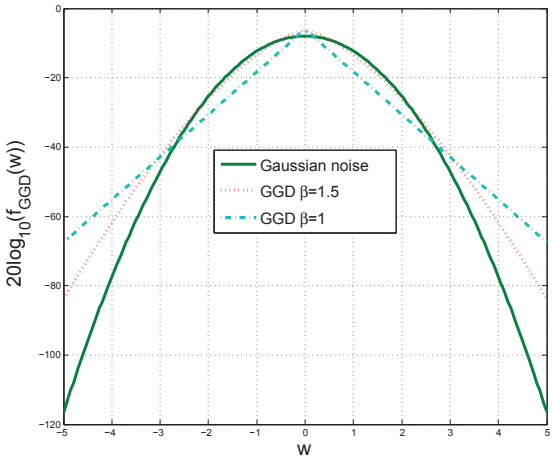

Fig. 2: PDF of GGD random variable for different β values and $\sigma_w^2 = 1$

The non-linear detector in [6], based on the Rao test, is optimized for GGD noise environments. As such, it can reduce the influence of high magnitude samples on the test statistic making it more reliable to indicate the presence or absence of a signal. The Rao test statistic can be formulated as:

$$T_R\{R_j(n)\} = \phi(\beta) \sum_{n=0}^{N-1} (|R_j^{\text{Re}}(n)|^{\beta'} + |R_j^{\text{Im}}(n)|^{\beta'}) \quad (8)$$

where $R_j^{\text{Re}}(n)$ and $R_j^{\text{Im}}(n)$ represent the real and imaginary parts of the receiver signal respectively, i.e., $R_j(n) = R_j^{\text{Re}}(n) + \jmath R_j^{\text{Im}}(n)$, $\beta' = 2(\beta-1)$, and

$$\phi(\beta) = \frac{\beta\Gamma(\frac{3}{\beta})^{\beta-1}}{(\beta-1)(\frac{\sigma_w^2}{2})^{\beta-1}\Gamma(\frac{1}{\beta})^{\beta-2}\beta\Gamma(1-\frac{1}{\beta})} \quad (9)$$

Similar to (4), the decision rule is given by:

$$T_R\{R_j(n)\} \underset{H_{0,j}}{\overset{H_{1,j}}{\gtrless}} \lambda_j \quad (10)$$

where λ_j is the decision threshold for the j^{th} subband. The test statistic $T_R\{R_j(n)\}$ is only a function of the shaping factor β, thereby requiring no *a priori* knowledge of the PU's signal, channel gains, or noise variance.

III. Incorporation into Multicarrier Structure

In this section, we incorporate the above detector for GDD noise environments into the UFMC scheme. To this end, we first describe the UFMC operation, and then explain how to implement the Rao-test based detection at the receiver end.

A. UFMC Operation

UFMC has recently attracted considerable attention due to its higher spectral efficiency and reduced intercarrier interference (ICI). In this approach, unlike OFDM, a filtering operation is applied to a group of consecutive subcarriers to minimize the potential interference from subcarriers of adjacent subbands. In the recent literature, slightly different implementations of the UFMC concept have been proposed [14]-[16]. The UFMC transceiver model that will be used in our work follows that of [14].

As seen from Fig. 3, at the transmitter, a group of K incoming complex data symbols are mapped into B subbands with index $j = 1,\ldots,B$, where each subband consists of $M = K/B$ tones with index $k = 0,\ldots,M-1$. The symbol affected to the k^{th} tone of the j^{th} subband is denoted as $X_{j,k}$. For each

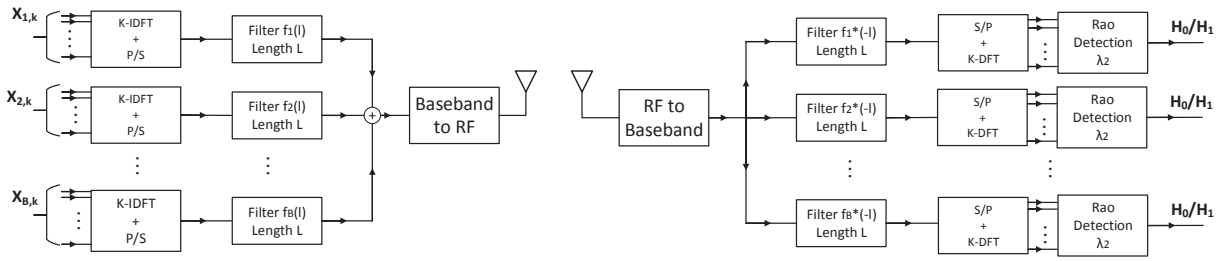

Fig. 3: System model of UFMC-based PU detection

subband, the corresponding time domain symbols $x_j(l)$ are obtained by applying a K-point IDFT spreader on $X_{j,k}$. More specifically, the group of tones in the j^{th} subband is offset by inserting θ_j zeros at the beginning; similarly, zeros are inserted at the end to account for unallocated subcarriers. In effect, this operation can be expressed as:

$$x_j(l) = \frac{1}{K} \sum_{k=0}^{M-1} X_{j,k} \mathrm{e}^{2\pi j l(k+\theta_j)/K} \tag{11}$$

where the index $l = 0, ..., K-1$ and $\theta_j = (j-1)M$. Each subband sequence $x_j(l)$ is passed through a corresponding finite impulse response (FIR) filter $f_j(l)$ of length L to reduce out-of-band leakage. Filter $f_j(l)$ is modulated to the proper frequency by multiplying a prototype impulse response $f(l)$ with an exponential sequence, that is: $f_j(l) = f(l)\mathrm{e}^{2\pi j l(\theta_j+(M-1)/2)/K}$. In this work, similar to [14], the $f(l)$ is obtained from a Dolph-Chebyshev window with adjustable sidelobe attenuation [18]. The output of the j^{th} subband after FIR filtering is expressed as:

$$y_j(l) = x_j(l) * f_j(l) = \sum_{l'=0}^{K-1} x_j(l') f_j(l-l') \tag{12}$$

where $*$ denotes the discrete-time convolution and the index $l = 0, \ldots, K+L-2$. The different subband signals $y_j(l)$ are then summed, resulting into

$$y(l) = \sum_{j=1}^{B} y_j(l) \tag{13}$$

Finally, the discrete-time baseband signal $y(l)$ is converted to an analog passband signal for transmission, via analog pulse-shaping and RF up-conversion.

Let $r(l)$ denote the baseband signal at the UFMC receiver front-end after RF down-conversion and sampling. For each one of the B subbands, the received signal $r(l)$ is convolved with the time reversal and complex conjugate of the corresponding subband filter $f_j(l)$. The resulting time-domain signal, denoted as $r_j(l)$, can be expressed as:

$$r_j(l) = r(l) * f_j^*(-l) = \sum_{l'=0}^{K+L-2} r(l') f_j^*(l'-l) \tag{14}$$

where only the samples with index $l = 0, ..., K-1$ are retained [14]. For each subband, the signal $r_j(l)$ is mapped to the frequency domain by applying a K-point DFT despreading operation. Specifically, the estimated symbol corresponding to the k^{th} tone of the j^{th} subband is expressed as:

$$R_{j,k} = \sum_{l=0}^{K-1} r_j(l) \mathrm{e}^{-2\pi j l(k+\theta_j)/K} \tag{15}$$

where the index $k = 0, \ldots, M-1$.

B. Incorporation of Rao Detector

For the wideband spectrum sensing model, we consider a multipath fading environment where $h(l)$ represents the baseband equivalent discrete-time impulse response of the radio channel between the PU and SU. That is, the signal at the UFMC receiver front-end of the SU can be written as:

$$r(l) = h(l) * y(l) + w(l) \tag{16}$$

where $y(l)$ is the PU signal component and $w(l)$ is the additive complex white noise with zero mean and variance σ_w^2. We note that the specific transmission scheme for the PU signal component $y(l)$ need not be known by the SU; that is, the PU may not necessarily employ UFMC or OFDM for transmission.

Following Section A, for a SU equipped with a UFMC-based receiver, the discrete-time signal $r(l)$ at the baseband front-end is filtered by subband filters $f_j^*(-l)$ for $j = 1, \ldots, B$. In the frequency domain, following the despreading operation, the received signal on the k^{th} tone of the j^{th} subband is then given by $R_{j,k}$ in (15).

We test the following binary hypotheses to decide whether the j^{th} subband, which consists of M tones with index $k = 0, 1, \ldots, M-1$, is accessible or not:

$$H_{0,j} : R_{j,k}(n) = W_{j,k}(n) \tag{17}$$

$$H_{1,j} : R_{j,k}(n) = H_{j,k}F^*_{j,k}(n)Y_{j,k}(n) + W_{j,k}(n) \tag{18}$$

for $n = 0, 1, \ldots, N-1$, where N is the total number of UFMC symbols in the given observation window. Here, $R_{j,k}(n)$ denotes the n^{th} estimated symbol on the k^{th} tone of the j^{th} subband, $H_{j,k}$ is the corresponding complex channel gain between the PU and SU, $F^*_{j,k}(n)$ is the K-point DFT of $f^*_j(-n)$, $Y_{j,k}(n)$ is the unknown PU signal component, and $W_{j,k}(n)$ is a GGD noise.

For each subband j, we compute the test statistic of the Rao detector over an interval of N symbols. Since a subband in UFMC consists of multiple tones or subcarriers, the test statistic for the j^{th} subband is obtained as the sum of the contributions from each symbol affected to the various tones with index k in that subband, assuming independent symbol sequences, and is formulated as:

$$T_R\{R_{j,k}(n)\} = \phi(\beta) \sum_{k=0}^{M-1} \sum_{n=0}^{N-1} (|R^{\text{Re}}_{j,k}(n)|^{2(\beta-1)} + |R^{\text{Im}}_{j,k}(n)|^{2(\beta-1)}) \tag{19}$$

for $k = 0, ..., M-1$. The decision rule is chosen as:

$$T_R\{R_{j,k}(n)\} \underset{H_{0,j}}{\overset{H_{1,j}}{\gtrless}} \lambda_j \tag{20}$$

where $R^{\text{Re}}_{j,k}(n)$ and $R^{\text{Im}}_{j,k}(n)$ represent the real and imaginary parts of $R_{j,k}(n)$, and λ_j is the decision threshold for the j^{th} subband.

IV. Numerical Simulations

In this section, we first describe the methodology used to simulate the UFMC-based wideband system for PU detection. We then show the sidelobe behavior for the UFMC and OFDM schemes to motivate the assumption that subband filtering improves detection performance. We obtain the ROC curves for UFMC with the Rao detector and energy detector and compare them to that of the OFDM system with both detectors. We also evaluate the effect of the non-Gaussianity level (shaping factor β) and the SNR on the detection performance.

A. Methodology

We consider a wideband spectrum sensing system with a PU transmitting OFDM symbols over 256 tones each carrying random QPSK data symbols. For simplicity, the transmitted signal has unit power, that is $E[|y(l)|^2] = 1$. We assume that the SU is equipped with a UFMC-based receiver, also with $K = 256$ tones. The signal at the receiver front-end is filtered by $B = 8$ subband Dolph-Chebyshev (DC) FIR filters of length $L = 74$ and with 35dB sidelobe attenuation. The filter coefficients $f(l)$ are chosen such that $\sum_{l=0}^{L-1} |f(l)|^2 = 1$. For the purpose of comparison, we also implement a system where the SU is equipped with an OFDM receiver with $K = 256$ tones.

In our experiments, we assume a Rayleigh fading channel consisting of 5 channel taps that does not vary over one observation window of N multicarrier symbols. The channel impulse response is normalized such that its energy $\sum_{n=0}^{4} |h(l)|^2 = 1$.

The noise in (16) is modeled as GGD with zero mean, variance σ_w^2, and parameter β. The samples are generated using the following procedure [19]:

- simulating a Gamma random variable $Z \sim$ Gamma (a,b) with parameter $a = \beta^{-1}$ and $b = (A(\beta, \sigma_w^2))^{-\beta}$;
- applying the transformation $Y = Z^{1/\beta}$;
- setting $w(l)$ to $\pm Y$ with probability of 0.5.

Under the previous normalization assumptions for the PU signal and channel, the SNR in dB is given as:

$$\text{SNR} = -10 \log_{10}(\sigma_w^2) \tag{21}$$

At the receiver of the system, data are collected over $N = 25$ vector symbols. Comparison of the detection performance is performed over the second subband (i.e. $j = 2$) where interference from neighboring subbands is present. In this way, we can compare UFMC and OFDM in terms of their robustness to out-of-band interference. The performance of the various detection algorithms under comparison is evaluated in terms of the probability of detection P_d and the probability of false alarm P_{fa}, as shown through parametric ROC curves. The ROC curves are obtained through Monte-Carlo simulations over 10^4 iterations.

B. Results and Discussion

We first show, in Fig.4, the sidelobe behavior of the second subband for the UFMC and OFDM receivers. As we expect, with added subband filtering at the receiver, UFMC has a better out of band rejection due its lower sidelobes. OFDM has high sidelobe levels resulting from the rectangular shape in time domain. This would indicate that the SU will be able to confine the spectral content of the transmitted signal within a subband when using UFMC.

We now show the simulated ROC curves of the Rao and energy detectors when integrated in the UFMC system and the OFDM system in presence of non-Gaussian noise with parameter $\beta = 1.1$. It can be observed, from Fig.5 that the Rao detector outperforms

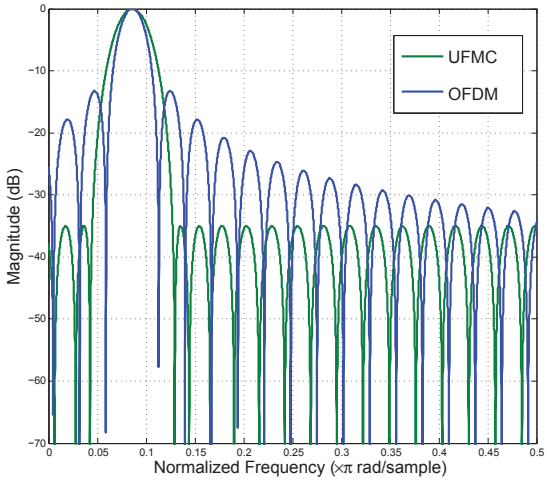

Fig. 4: Sidelobe behavior of UFMC and OFDM

the energy detector when the background noise is non-Gaussian, and this for both UFMC and OFDM receiver schemes. Indeed, given a P_{fa} of 0.1, there is a 55% increase of P_d for the Rao detector over the energy detector in the OFDM system and 37% in the UFMC scheme. Moreover, it can be seen that with the use of filters in the UFMC scheme, SUs detect better the presence of a PU in a given band over the OFDM scheme. We can observe from the figure that given a P_{fa} of 0.1, the Rao detector in the UFMC system surpasses the Rao detector in the OFDM system by 14%.

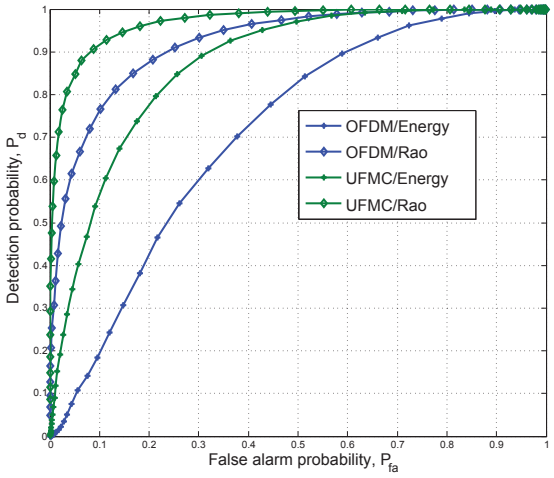

Fig. 5: ROC curves of the Energy and Rao detectors integrated in UFMC and OFDM for $\beta = 1.1$ and SNR = -10dB

Fig. 6 shows the effects of the noise shaping factor β on the ROC curves of the energy and Rao detectors integrated in the UFMC system. We can see that, as β decreases or the non-Gaussianity of the noise increases, the P_d rises. This is not the case for the energy detector, where as β decreases or the non-Gaussianity of the noise increases, the P_d drops. This means that SUs will be able to detect the PU signal more effectively, when using the Rao detector over the energy detector, in practical non-Gaussian noise environments which tend to exhibit probability density functions with tails decaying at lower rates than the traditional Gaussian density tails (i.e. shaping factor $\beta < 2$).

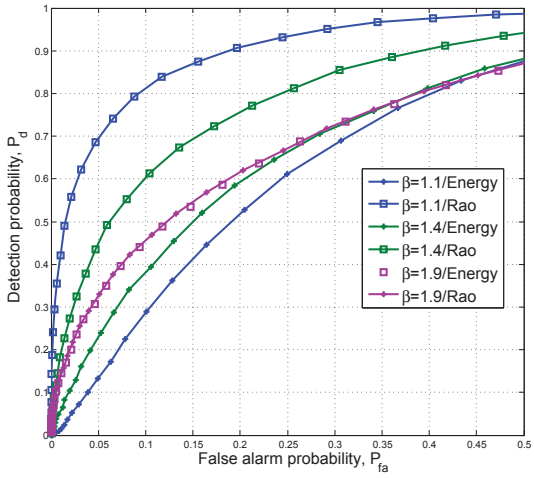

Fig. 6: Effect of GGD noise shaping factor β on ROC curve for Rao dector integrated in UFMC for SNR = -20dB

In Fig. 7, the ROC curves of the Rao and energy detectors incorporated in the UFMC system for different SNRs are shown. As expected, the detection performance of the Rao detector is reduced as the SNR is reduced and is much better than with the energy detector for all values of SNR.

V. Conclusion

In this paper, we investigated the performance of the Rao-test based detector for wideband spectrum sensing under non-Gaussian noise in a multi-carrier transmission framework. Specifically, we incorporated this detector into the universal filtered multicarrier (UFMC) modulation scheme envisaged for 5G systems. Through numerical simulations, we showed that the Rao-test based detector combined with UFMC outperforms the traditional OFDM based system in a realistic non-Gaussian noise environment. An interesting avenue for future work will be to investigate the optimal threshold selection for all subbands in a joint manner as in [8].

VI. References

[1] T. Yucek and H. Arslan, "A survey of spectrum sensing algorithms for cognitive radio applications," *Commun. Surveys Tuts*, vol. 11, no. 1, 2009, pp. 116-130.

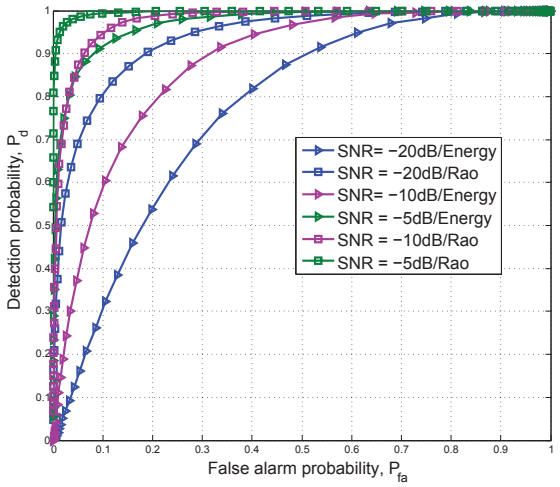

Fig. 7: Effect of SNR (dB) on ROC curve of the Rao detector integrated in UFMC and OFDM for $\beta = 1.1$

[2] FCC Spectrum Policy Task Force ET Docket No. 02-135, Nov. 2002.

[3] D. Bhargavi and C. R. Murthy, "Performance comparison of energy, matched-filter and cyclostationarity-based spectrum sensing," *in Proc. IEEE Workshop on Signal Advances in Wireless Commun.*, June 2010, pp. 1-5.

[4] J. K. Tugnait and G. Huang, "Cyclic autocorrelation based spectrum sensing in colored Gaussian noise," *in Proc. IEEE Wireless Commun. Netw. Conf.*, Paris, France, Apr. 1-4, 2012, pp. 731-736.

[5] R. Umar, A. U. H. Sheikh, and M. Deriche, "Unveiling the hidden assumptions of energy detector based spectrum sensing for cognitive radios," *Commun. Surveys Tuts*, vol. 16, no. 2, 2014, pp. 713-728.

[6] X. Zhu, B. Champagne, and W. P. Zhu, "Rao test based cooperative spectrum sensing for cognitive radios in non-Gaussian noise," *Signal Process.*, vol. 97, April 2014, pp. 183-194.

[7] H. Sun, A. Nallanathan, C.-X. Wang, and Y. Chen, "Wideband spectrum sensing for cognitive radio networks: A survey," *IEEE Wireless Commun.*, vol. 20, no. 2, April 2013, pp. 74-81.

[8] Z. Quan, S. Cui, and A. Sayed, H. Poor, "Optimal multiband joint detection for spectrum sensing in cognitive radio networks," *IEEE Trans. on Signal Process. 57*, March 2009, pp.1128-1140.

[9] K. Hossain, B. Champagne, and A. Assra, "Cooperative multiband joint detection with correlated spectral occupancy in cognitive radio networks," *IEEE Trans. on Signal Process.*, vol. 60, no. 5, May 2012, pp. 2682-2687.

[10] P. Banelli, S. Buzzi, G. Colavolpe, A. Modenini, F. Rusek, and A. Ugolini, "Modulation formats and waveforms for 5G networks: Who will be the heir of OFDM?: An overview of alternative modulation schemes for improved spectral efficiency," *IEEE Signal Process. Mag.*, vol. 31, no. 6, Nov. 2014, pp. 80-93.

[11] G. Cherubini, E. Eleftheriou, and S. Olcer, "Filtered multitone modulation for very high-speed digital subscriber lines," *IEEE J. Select. Areas Commun.*, vol. 20, no. 5, June 2002, pp. 1016-1028.

[12] N. Zhao, F. Pu, X. Xu, and N. Chen, "Cognitive wideband spectrum sensing using cosine-modulated filter banks," *Int. J. Electron.*, vol. 102, no. 11, 2015, pp. 1890-1901.

[13] P. Siohan, C. Siclet, and N. Lacaille, "Analysis and design of OFDM-OQAM systems based on filterbank theory," *IEEE Trans. Signal Process.*, vol. 50, no. 5, May 2002, pp. 11701183.

[14] V. Vakilian, T. Wild, F. Schaich, S. ten Brink, and J.-F. Frigon, "Universal-filtered multi-carrier technique for wireless systems beyond LTE," *Proc. IEEE GLOBECOM Broadband Wireless Access Workshop*, Dec. 2013, pp. 223-228.

[15] F. Schaich and T. Wild, "Waveform contenders for 5G - OFDM vs. FBMC vs. UFMC", *Proc. of 6th Int. Symp. on Commun., Control, and Signal Process.*, Athens, Greece, May 2014, pp.457-460.

[16] X. Wang, T. Wild, F. Schaich, and A. Santos, "Universal Filtered Multi-Carrier with Leakage-Based Filter Optimization," *European Wireless*, Barcelona, May 2014, pp.963-967.

[17] S.A. Kassam, *Signal Detection in Non-Gaussian Noise*, Springer Verlag, 1988.

[18] A. Antoniou, *Digital Filters*, McGraw-Hill, 2000.

[19] M. Nardon and P. Pianca, "Simulation techniques for generalized Gaussian densities," Department of applied mathematics, University of Venice, Working Paper no. 145/2006, November 2009.